Doping of ceria surfaces with lanthanum: a DFT + U study

Doping of ceria surfaces with lanthanum: a DFT + U study

Irene Yeriskin and Michael Nolan

Tyndall National Institute, University College Cork, Lee Maltings, Prospect Row, Cork,
Republic of Ireland

E-mail: michael.nolan@tyndall.ie

Abstract

In this paper we use density functional theory corrected for on-site Coulomb interactions
(DFT + U) to study the defects formed in the ceria (111) and (110) surfaces doped with La. To
describe consistently the defect formed with substitutional La^{3+} doping at a Ce^{4+} site we use
DFT and DFT + U, with $U = 5$ eV for Ce 4f states and $U = 7$ eV for O 2p states. When La^{3+}
substitutes on a Ce^{3+} site, an $La'_{Ce} + O^{\cdot}_O$ defect state, with an oxygen hole, is formed at both
surfaces, but only with the DFT + U approach. The formation energy of an oxygen vacancy in
a structure with two La dopants in their most stable distribution is reduced over the undoped
surfaces but remains positive. Formation of an oxygen vacancy results in the appearance of a
reduced Ce^{3+} cation and a compensated oxygen hole, instead of compensation of both oxygen
holes, which is typical of metal oxides doped with lower valence cations. We tentatively suggest
that the key role in the formation of this unusual defect is played by cerium and arises from the
ease with which cerium can be reduced, as compared to other metal oxides. Experimental
confirmation of these results is suggested.

S Online supplementary data available from stacks.iop.org/JPhysCM/22/135004/mmedia

(Some figures in this article are in colour only in the electronic version)

1. Introduction

Cerium oxide (ceria) is of importance in a number of
fields, such as oxidation–reduction (redox) catalysis [1, 2],
intermediate temperature solid oxide fuel cells [3] and gas
sensing [4]. In each of these areas, the formation (and
migration) of oxygen vacancies plays a key role. Ceria already
has a relatively small oxygen vacancy formation energy, which
has its origin in the ease with which cerium can change
oxidation state from (formally) +4 to (formally) +3. This
property of ceria makes it an active material in catalytic
reactions such as oxidation of CO to CO_2 and reduction of
NO_X to N_2.

Nanostructures of ceria such as nanorods [5] and
nanoparticles [6] have been well studied in recent years and
there is some modelling work on nanoparticles of ceria. In
brief, the evidence is that the reactivity of a nanostructure
appears to depend on its shape—for the example of CO
oxidation, nanorods are more reactive than nanoparticles [7].
The origin for this lies in the crystal faces that are exposed on
these structures. Nanoparticles expose primarily (111) faces,
while nanorods expose primarily (110) faces. First principles
computations of CO adsorption at the (111) and (110) surfaces
(which are reasonable models of the exposed crystal faces in
the nanostructures) show that there is no interaction of CO with
the (111) surface and a strong interaction of CO at the (110)
surface [8–10]. The origin of the different relativities to CO
was attributed to the structure of the surface and the relative
oxygen vacancy formation energy [9].

Given that the (111) surface is the most stable surface
of bulk ceria [11] and is predominant in nanoparticles, it is
worth investigating how the reactivity of this surface can be
enhanced. To briefly recall, the oxygen vacancy formation
energies of the low index surfaces of ceria increase in the
order (110) < (100) < (111) [12] and thus lowering the
oxygen vacancy formation energy of ceria should be a means of
enhancing the reactivity. In fact, it is now clear that doping of
ceria with other metal cations is one potentially fruitful means
of achieving this enhancement [13–18]. Recent experimental
work has shown that many metal dopants enhance the oxygen
vacancy formation energy and reactivity of ceria. In parallel,
there have been a number of modelling studies of metal

doping of ceria bulk and surfaces, which also show a reduced oxygen vacancy formation energy [19–25]. In [19, 25] the authors provided explanations for the reduction in the vacancy formation energy of ceria upon doping.

While trivalent rare earths such as Eu^{3+} have recently been shown to enhance the oxidation of CO to CO_2 [17], there has been relatively little work on La doping of ceria [17, 26]. In this paper, we apply first principles density functional theory, corrected for on-site Coulomb interactions (DFT+U) [27, 28], to study La doping of ceria. In the modelling, we study La doping of the (111) and (110) ceria surfaces. The (111) surface is by far the most well studied surface of ceria and is predominantly present in nanoparticles [6], while (110) is the more reactive surface [12] and is present on structures such as nanorods [5]. The DFT + U approach has been shown to provide a consistent treatment of reduced Ce ions in ceria, e.g. [11, 12, 29, 30]. In this approach, the value of U must be somehow chosen; our earlier work arrived at $U = 5$ eV, based on comparison of the photoemission spectrum of reduced ceria [31] and the computed density of states [10] and we choose it for this work. We show that localized hole formation in La-doped ceria needs to be described by DFT+U, with U on O 2p states (to be elaborated upon in the following sections) and that oxygen vacancy formation does not lead to hole compensation, but instead to formation of reduced Ce^{3+} simultaneously present with an oxygen hole in the surface.

2. Computational methods

We use a slab model of the ceria (111) and (110) surfaces and a plane wave basis set to describe the valence electronic wave functions with the VASP code [32]. The cut-off for the kinetic energy is 396 eV. For the core–valence interaction we apply Blöchl's projector augmented wave (PAW) approach [33]. For Ce, we use 12 valence electrons, for La 11 valence electrons and for O a [He] core. We use the Perdew–Burke–Ernzerhof (PBE) approximation for the exchange–correlation functional [34]. In common with earlier studies [10, 11, 29, 30], we use density functional theory (DFT) corrected for on-site Coulomb interactions (DFT + U), where $U^{Ce4f} = 5$ eV and is applied to the Ce 4f states. The details of this approach and our choice of U are discussed extensively in [10, 11]. k-point sampling is performed using the Monkhorst–Pack scheme, with a $(2 \times 2 \times 1)$ sampling grid.

The (111) surface is type II (in the Tasker classification) with neutral, stoichiometric O–Ce–O units along the slab and no dipole moment is present upon cleaving [35], while the (110) surface is of type I, with neutral CeO_2 planes along the slab. For the (111) surface, we use a (4×4) expansion of the surface supercell in which one dopant gives an overall doping level of 1.6% with a 3.2% doping concentration for two La dopants. For the (110) surface, a (4×2) expansion of the surface cell is used, in which one dopant gives an overall doping level of 1.8% for one La dopant and 3.6% for two La dopants. Formation of one oxygen vacancy gives an overall oxygen vacancy concentration of 0.8% in the (111) surface and 0.9% in the (110) surface. The slab models are 4 O–Ce–O layers (11.5 Å) thick for (111) and 7CeO_2 layers (11.5 Å)

thick for (110), with a 15 Å vacuum gap and the bottom two layers were fixed during the relaxations. All calculations are spin polarized with no restrictions on the overall spin.

It is well known that substituting an M^{n+} cation in a metal oxide with a lower valence $M^{(n-1)+}$ cation results in formation of a localized electronic hole on an oxygen atom neighbouring the dopant [36–43]. This electronic hole gives rise to issues with the description of the resulting electronic structure using DFT, which we, for example, have discussed in detail for Li-doped MgO and Si-doped Al_2O_3 [44, 45]; see also [46, 47] for detailed treatments of the latter system and discussions of this problem.

In the present example, substitution of Ce^{4+} with La^{3+} results in formation of an $La'_{Ce} + O_O^{\bullet}$ defect centre, with an oxygen hole, formed by occupation of one O 2p orbital with one electron (rather than two electrons) or formation of two $La'_{Ce} + O_O^{\bullet}$ centres compensated by an oxygen vacancy. For the example of Li-doped MgO [44] and Al-doped SiO_2 [45], we previously demonstrated that the description of these defects using DFT+U, with U applied to the O 2p states, is consistent with experiment. The choice of $U^{O\ 2p}$ is 7 eV, which can also be arrived at from experiment [48]. In addition, with $U = 7$ eV on O 2p states in MgO, we have found that oxygen vacancies compensate the electronic holes [49], giving further confidence in using this approach for these doped systems. For comparison, we also present some calculations with no U on oxygen.

To see the impact of using DFT + U on oxygen 2p states, we discuss briefly how thermodynamics are influenced. Firstly, we consider the binding energy of the O_2 molecule, which is notoriously difficult to describe accurately with DFT [50]. Indeed we find that with no U on O 2p, the O_2 binding energy is overestimated by 1.4 eV. With $U = 7$ eV on O 2p, the computed binding energy of 4.91 eV is rather close to the experimental data, which show a range of 5.08–5.16 eV [50]. Thus, the use of U on O 2p states can be expected to be suitable for thermodynamics. For the oxides, we compute the formation energy of CeO_2 to be −11.84 eV, which is in reasonable agreement with experimental data [1, 51]. The formation energy of one oxygen vacancy in the (110) surface used in this paper is computed to be 1.18 eV, which compares with 1.58 eV for no U on oxygen. As we have discussed in [11] and [45], we find that DFT + U tends to give energies, such as oxygen vacancy formation energies, that are around 0.3–0.4 eV lower than DFT and our result here is quite consistent with this.

The formation energy of an oxygen vacancy in doped ceria is given by (for the example of the (111) surface)

$$E^{vac} = [E(La_{0.016}Ce_{1.984}O_{1.992}) + E(1/2O_2)]$$
$$- E(La_{0.016}Ce_{1.984}O_2) \quad (1)$$
$$E^{2vac} = [E(La_{0.016}Ce_{1.984}O_{1.984}) + E(1/2O_2)]$$
$$- E(La_{0.016}Ce_{1.984}O_{1.992}) \quad (2)$$

with the dopant and vacancy concentrations calculated from the subscripts on La and O in (1) and (2); the latter equation is for formation of two oxygen vacancies. The energy of O_2 is computed using $U^{O\ 2p} = 7$ eV for those calculations in which $U^{O\ 2p}$ is used on the oxide. Throughout this paper, a negative energy signifies that formation of an oxygen vacancy is favourable.

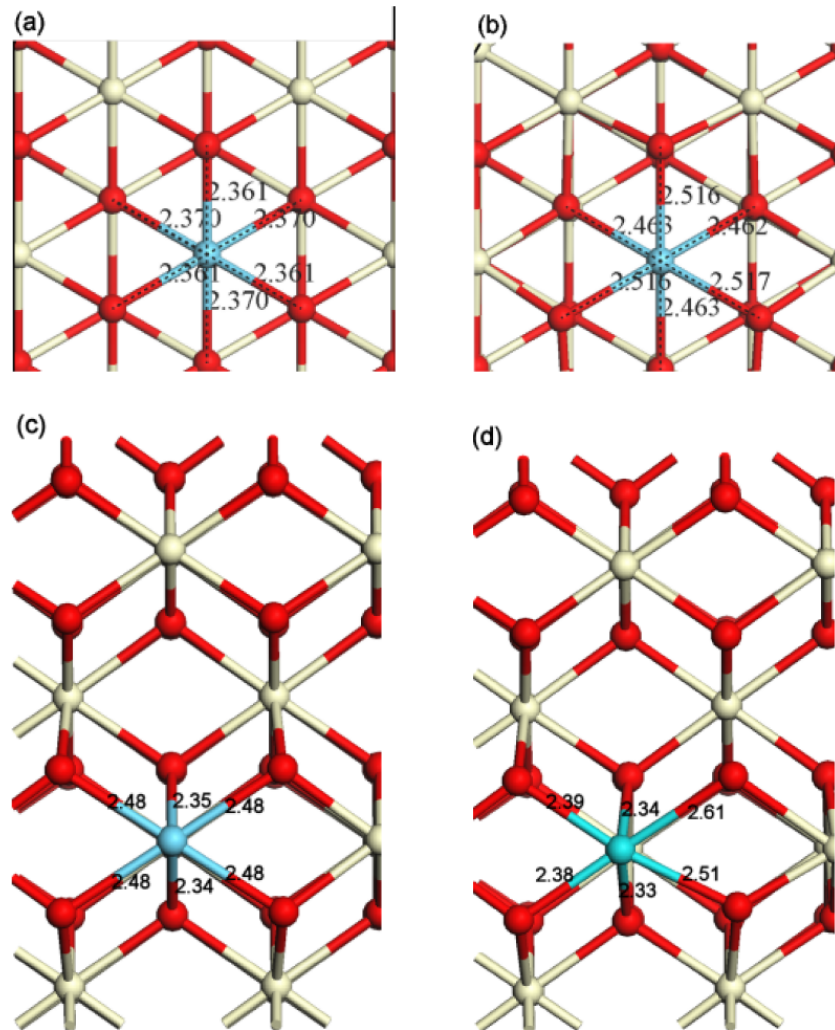**Figure 1.** (a) Geometry of La-doped $CeO_2(111)$ with no U on oxygen (b) with $U^{O\ 2p}$ on oxygen. (c) Geometry of La-doped $CeO_2(110)$ with no U on oxygen and (d) with $U^{O\ 2p}$ on oxygen. In this and in subsequent figures, cerium is grey (white in print), oxygen is red (black in print) and lanthanum is blue (grey in print). This figure shows a portion of the surface around the dopant site and the La–O distances are given in Å.

3. Results and discussion

3.1. The atomic structure of La-doped ceria surfaces

We begin by describing the atomic structure of the ceria (111) and (110) surfaces with the introduction of one La dopant. The supplemental information (available at stacks.iop.org/JPhysCM/22/135004/mmedia) provides the atomic coordinates of various doped structures presented in this paper. In the undoped (111) surface, the surface Ce–O distances are equivalent (2.36 Å), and subsurface Ce–O distances are similar to bulk. This surface is the most stable ceria surface and undergoes little relaxation; the stability of the (111) surface is the origin of its relative lack of reactivity compared to other ceria surfaces, such as (110), e.g. for CO adsorption [8]. The (110) surface has stoichiometric CeO_2 plane along the slab and the in surface layer, Ce–O distances are 2.34 and 2.32 Å to the first subsurface layer.

The geometry of the La-doped $CeO_2(111)$ surface is shown for a region around the dopant in figure 1(a) for a calculation with no U on oxygen and in figure 1(b) for a

calculation with $U^{O\ 2p}$ on oxygen. The La–O distances are given in each figure. There is an immediate difference between the two computational approaches in terms of the geometry. With no U on oxygen, there are two sets of La–O distances, three at 2.36 Å and another three at 2.37 Å; the former La–O distances involve terminating surface oxygen atoms and the latter distances involve subsurface oxygen atoms and both are rather similar to the Ce–O distances in the surface. Thus, the La–O distances are quite uniform. However, with $U^{O\ 2p}$, there is a notable distortion present. The La–O distances to terminal oxygen atoms elongate to 2.52 Å, while to subsurface oxygen atoms, the La–O distances are 2.46 Å. These La–O distances are substantially elongated compared to the Ce–O distances in the undoped surface, with the stronger elongation to the terminal oxygen atoms.

In the La-doped (110) surface, similar differences between the DFT approaches are found. With no U on oxygen, there are 4 La–O distances of 2.48 Å involving surface O and two of 2.34/2.35 Å. The presence of the large La ion forces longer cation–O distances in the vicinity of the dopant. With U
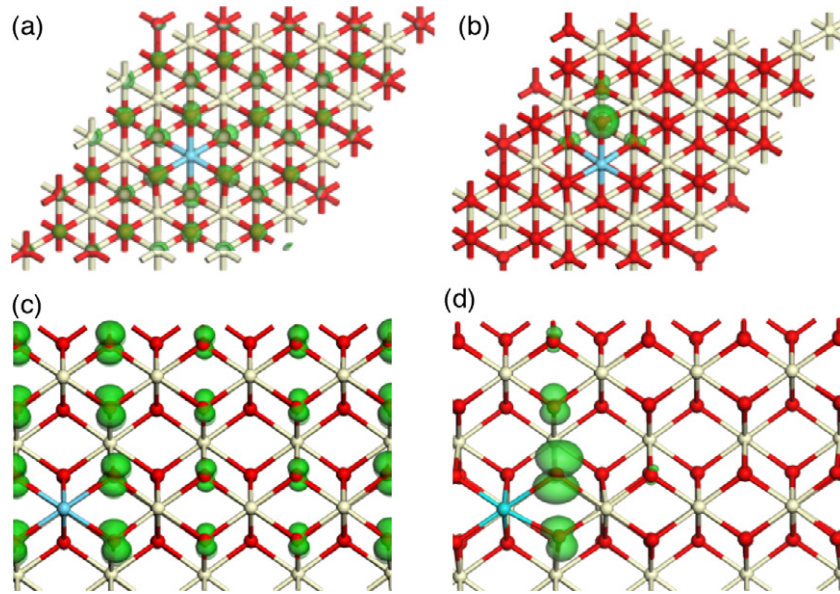
Figure 2. (a) Excess spin density isosurfaces for La-doped $CeO_2(111)$ with no U on oxygen (b) with $U^{O\ 2p}$ on oxygen. (c) Geometry of La-doped $CeO_2(110)$ with no U on oxygen and (d) with $U^{O\ 2p}$ on oxygen. In this and in subsequent figures, cerium is grey (white in print), oxygen is red (black in print) and lanthanum is blue (grey in print).
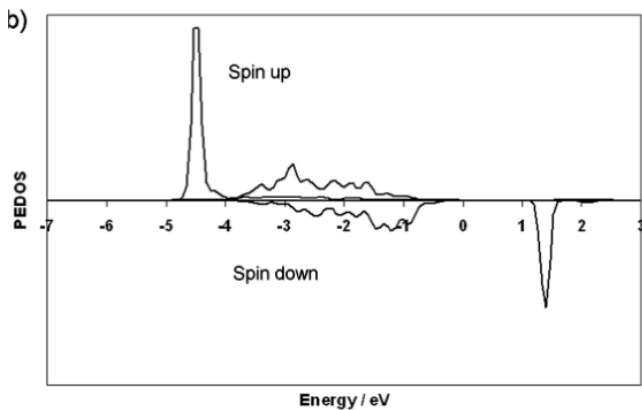

Figure 3. Electronic density of states projected on O 2p states for La-doped $CeO_2(111)$ surface with U on oxygen for the hole-carrying oxygen in figure 2.

on oxygen, there is a strong distortion—there is one strongly elongated surface La–O distance of 2.61 Å and another at 2.51 Å; the remaining two surface La–O distances are reduced to 2.38/2.39 Å, consistent with the La cation moving away from one pair of surface oxygen atoms, thus shortening the distance to the other pair of surface oxygen atoms.

3.2. Electronic structure of La-doped CeO₂ surfaces

To investigate the destination of the oxygen hole, we plot the excess spin density (difference between up and down spin electron density) in both La-doped surfaces in figure 2. Upon comparing the spin density for either surface with no U on oxygen and with U on oxygen, there is an immediate difference between the two descriptions. With no U on oxygen, the hole is delocalized over terminal and subsurface oxygen atoms of

the surface, with computed spin magnetizations of 0.01–0.05 electrons on oxygen, with the largest spin magnetization on oxygen nearest the dopant. With $U^{O\ 2p}$, the spin density is strongly localized on one surface terminating oxygen near the dopant, with computed spin magnetizations of 0.93 electrons on the (111) surface and 0.95 electrons on the (110) surface, with a very small spin density on some neighbouring oxygen atoms. On both surfaces, the hole is localized on an oxygen atom with the longest surface La–O distance, 2.52 Å on (111) and 2.61 Å on (110). The predominant localization of the hole on one oxygen atom near the dopant is consistent with the behaviour for other similar systems [36–47].

The partial electronic density of states (PEDOS) projected on O 2p states for the oxygen atom that carries the electronic hole for the example of La-doped $CeO_2(111)$ with U on O 2p is shown in figure 3. In the PEDOS we see firstly that there are no Ce 4f derived gap states in the band gap, confirming no reduced Ce^{3+} ions are present. Secondly, the PEDOS shows two peaks of significance. The first is 4.5 eV below the Fermi level, in the valence band region, and the second is at 1.3 eV above the Fermi level (set at 0 eV). This is consistent with the formation of a localized O^- species; a delocalized O^- species shows a very different PEDOS structure. Based on previous work on Li-doped MgO [52], it could be possible to use electron energy loss spectroscopy to establish the position of the oxygen hole in the electronic structure. Throughout the remainder of this paper we will work with the DFT + U approach with U on oxygen.

3.3. Oxygen vacancy formation

To investigate if the compensated defect formed when $2La'_{Ce} + O^{\bullet}_O$ holes are accompanied by a single oxygen vacancy, which is the classical defect compensation mechanism, is more
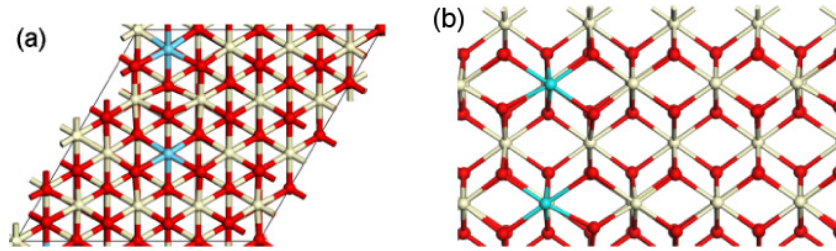
Figure 4. (a) Distribution of two La dopants in the (111) surface in their most stable configuration, with a 6.70 Å separation. (b) Distribution of two La dopants in the (110) surface in their most stable configuration, with a 5.47 Å separation. The colour scheme is the same as figure 1.
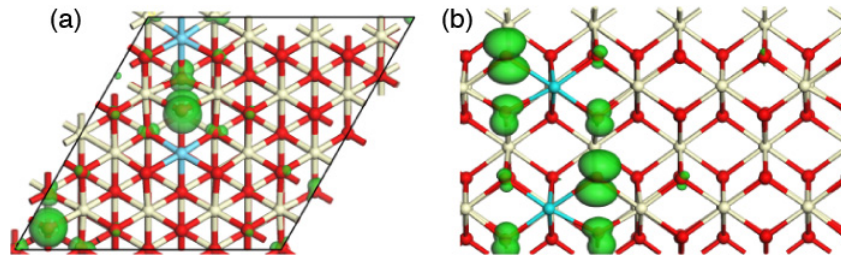

Figure 5. (a) Excess spin density for 2 La dopants in the (111) surface. (b) Excess spin density for 2 La dopants in the (110) surface. The colour scheme is the same as figure 1 and the isosurface contours are 0.01 electrons Å^{-3}.

stable than the uncompensated defect, we investigate two 2La dopants incorporated into the ceria surfaces and the formation of an oxygen vacancy.

For two La dopants at each surface, there are a number of possible distributions. For the (111) surface, the La–La distribution shown in figure 4(a), in which the dopants are separated by 6.70 Å, is the most stable. For the (110) surface, the La–La distribution in figure 4(b), in which the dopants are separated by 5.47 Å, is the most stable. The geometry around the dopants on each surface is similar to the case for a single La dopant. At the (111) surface, this gives La–O distances of 2.52 Å to terminal oxygen atoms and 2.46 Å to subsurface oxygen atoms. On the (110) surface, this results in two surface La–O distances of 2.60 Å and 2.50 A to one pair of surface oxygen atoms (very similar to one La dopant in the surface) and two surface La–O distances of 2.41 Å.

The spin density plots in figure 5, computed with U on oxygen, show prominent localization of the two oxygen holes at two oxygen atoms, each coordinated to one dopant. The computed spin magnetizations are 0.93 electrons per oxygen on (111) and 0.94 electrons per oxygen on (110). Again, these are the surface oxygen atoms with the longest La–O distances. In essence, these dopant distributions provide two isolated La dopants and oxygen holes.

Next, we remove an oxygen atom from these dopant structures and compute the oxygen vacancy formation energy—if this quantity is negative, then the vacancy forms to compensate the dopants, otherwise, the stable defect is the $La'_{Ce} + O^{\bullet}_{O}$ hole. The main oxygen sites that are considered for the vacancy in the (111) surface are shown in figure 6, along with their computed oxygen vacancy formation energies. All oxygen vacancies show an energy cost, while that of dopant–vacancy distribution I is the lowest, at 0.90 eV. These energies do indicate that an oxygen vacancy will not necessarily form

to compensate for the formation of the electronic hole state. At the same time, a formation energy of 0.90 eV is much reduced over the undoped surface (computed to be 2.60 eV [12]) and suggests that formation of this oxygen vacancy will be enhanced over the undoped surface.

Figure 7(a) shows the geometry around the vacancy site for the most stable oxygen vacancy on the (111) surface, with the vacancy indicated by a black 'V'. Similar to the undoped (111) surface, formation of a surface oxygen vacancy results in a breaking of the hexagonal symmetry of the terminating oxygen and the hexagon (with two surface Ce and one La dopant) is now distorted. The Ce–O distances in the hexagon are 2.31 Å to surface oxygen and 2.29 Å to subsurface oxygen. There is a shortening of the La–O distances to 2.46 Å to surface oxygen and no change in the La–O distances to subsurface oxygen.

On the (110) surface, the most stable oxygen vacancy site is shown in figure 7(c); the missing oxygen atom was coordinated to La and there is an energy cost of 0.64 eV to form this vacancy, which is strongly reduced over the undoped surfaces. In this structure, the surface oxygen atoms neighbouring the vacancy site move towards the vacancy, distorting the structure around the vacancy site and shortening the surface La–O distances to 2.33–2.32 Å. Surface Ce–O distances around the vacancy site are now similar to those in the undoped surface, suggesting that vacancy formation has released some of the distortions present in the surface after La doping.

Figures 7(b) and (d) show the resulting spin density for the oxygen vacancy structures. The most stable spin magnetization is with an excess of two up spin electrons, and the spin density plot reflects this. The spin density on both surfaces shows one electronic hole on a surface oxygen atom near one La dopant and, unexpectedly, a reduced subsurface Ce^{3+} ion near the
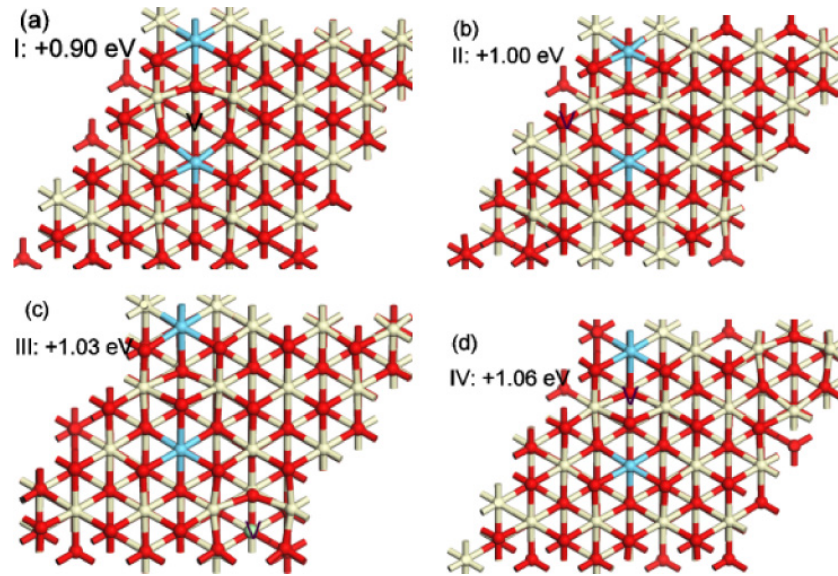
Figure 6. Oxygen vacancy sites on $CeO_2(111)$ surface with two La dopants. The energies given are the formation energy for each vacancy and the vacancy site is indicated with a black 'V'.
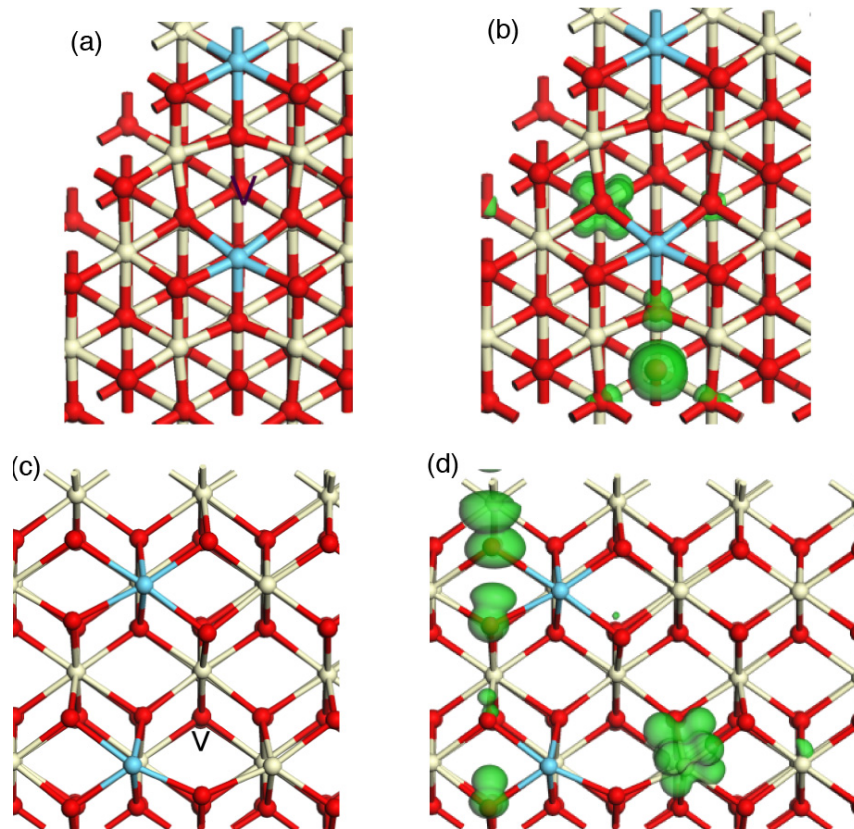

Figure 7. (a) Geometry around the vacancy site for the most stable dopant–vacancy distribution in the La-doped (111) surface. (b) Excess spin density plot for the most stable dopant–vacancy distribution in the La-doped (111) surface. (c) Geometry around the vacancy site for the most stable dopant–vacancy distribution in the La-doped (110) surface. (d) Excess spin density plot for the most stable dopant–vacancy distribution in the La-doped (110) surface. In parts (a) and (c), we show a portion of the full surface.

other La dopant on the (111) surface and a reduced surface Ce^{3+} ion on the (110) surface. This reduced Ce^{3+} species has an elongated Ce–O distance of 2.44 Å to the nearest subsurface oxygen and a small elongation of other Ce–O distances to 2.38 Å on the (111) surface. The presence of the Ce^{3+} ion in the subsurface layer on the (111) surface is consistent with recent results on oxygen vacancy formation on the undoped surface [53].

The finding that oxygen vacancy formation on ceria surfaces doped with La results in formation of Ce^{3+} and an oxygen hole seems at first surprising, since it is generally accepted that the formation of an oxygen vacancy defect compensates an aliovalent dopant with a lower oxidation state; for example, in Li-doped MgO (even with $U = 7$ eV on O 2p states), oxygen vacancy formation always compensates the two electronic holes [49]. For TiO_2 Islam et al showed that an Al dopant is compensated with an oxygen vacancy [54]. A UV–visible spectroscopy study of TiO_2 substitutionally doped with Al found that oxygen vacancies compensate the oxygen hole [55]. On the basis of the limited experimental information and the results in [54], it was concluded that Al-doped TiO_2 will be found with oxygen vacancies. A further experimental example is trivalent doped zirconia in [41] and [42], where oxygen vacancies are found to compensate the oxygen hole introduced by the dopant. In these examples, we see that hole compensation is favoured over cation reduction, even though TiO_2 is considered a reducible oxide. We suggest that new experiments are needed to study this area is more detail.

With no experimental information available to compare with our findings, we tentatively suggest that our results can be best understood when we consider the nature of the host oxide. In MgO, Mg is not reducible upon formation of an oxygen vacancy and forms instead F-centres, which are localized at the vacancy site. Upon doping with Li, the formation of an oxygen vacancy will not reduce Mg and results in hole compensation. Similarly, Zr in zirconia is not easily reducible and oxygen vacancy formation is trivalent doped zirconia will not reduce the Zr cation. The few experimental data for Al-doped TiO_2 suggest that Ti reduction is less favourable than compensation of the oxygen hole.

Cerium however is more easily reduced compared to the oxides listed above, and formation of an oxygen vacancy (with an appropriate value of U on Ce, as in the present paper) results in formation of reduced Ce^{3+}. In the absence of experimental information on this aspect of La-doped ceria, we tentatively propose that the energetics of cerium reduction mean that upon oxygen vacancy formation, it is favourable to reduce one Ce^{4+} ion to Ce^{3+} and compensate one oxygen hole, rather than compensate both electronic holes as in other oxides. Thus we propose that the key role in determining the defects formed upon La doping of ceria is played by the cerium cation. The remaining vacancy distributions that we considered show the same behaviour. Experimental work to elucidate the nature of the oxidation states of Ce and O in La-doped CeO_2 would be valuable to test these findings.

4. Conclusions

When the (111) and (110) ceria surfaces are doped with La, the most stable defect is $La'_{Ce} + O^{\cdot}_O$ with an oxygen hole. The formation of an oxygen hole is confirmed from structural and electronic data. We compute that the energy required to form an oxygen vacancy in this structure is at least 0.90 eV on (111) and 0.64 eV on (110), which is small enough that vacancy formation will be enhanced over the undoped surface and under favourable temperature and conditions, reduced Ce^{3+} ions can

be present. Perhaps the most interesting finding is that oxygen vacancy formation does not compensate the electronic holes, but instead compensates one hole and produces one Ce^{3+} ion, so that both electronic holes and Ce^{3+} ions can be present in La-doped ceria.

References

[1] Trovarelli A 2002 *Catalysis by Ceria and Related Materials* (London: Imperial College Press)
[2] Trovarelli A 1996 *Catal. Rev.—Sci. Eng.* **38** 439
[3] Goodenough J B and Huang Y H 2007 *J. Power Sources* **173** 1
[4] Izu N, Nishizaki S, Itoh T, Nishibori M, Shin W and Matsubara I 2009 *Sensors Actuators* B **136** 364
[5] Liu X W, Zhou K B, Wang L, Wang B Y and Li Y D 2009 *J. Am. Chem. Soc.* **131** 3140
[6] Huang X S, Sun H, Wang L C, Liu Y M, Fan K N and Cao Y 2009 *Appl. Catal.* B **90** 224
[7] Zhou K B, Wang X, Sun X M, Peng Q and Li Y D 2005 *J. Cataly.* **229** 206
[8] Yang Z X, Woo T K, Baudin M and Hermansson K 2004 *Chem. Phys. Lett.* **396** 384
[9] Nolan M and Watson G W 2006 *J. Phys. Chem.* B **110B** 16600
[10] Huang M and Fabris S 2008 *J. Phys. Chem.* C **112C** 8643
[11] Nolan M, Grigoleit S, Sayle D C, Parker S C and Watson G W 2005 *Surf. Sci.* **576** 217
[12] Nolan M, Parker S C and Watson G W 2005 *Surf. Sci.* **595** 223
[13] Patl S, Seal S, Guo Y, Schulte A and Norwood J 2006 *Appl. Phys. Lett.* **88** 243110
[14] Ou D R, Mori T, Ye F, Kobayashi T, Zuo J, Auchterlonie G and Drennan J 2006 *Appl. Phys. Lett.* **89** 171911
[15] Dutta G, Waghmare U V, Baidya T, Hegde M S, Priolkar K R and Sarode P R 2006 *Catal. Lett.* **108** 165
[16] Dutta G, Waghmare U V, Baidya T, Hegde M S, Priolkar K R and Sarode P R 2006 *Chem. Mater.* **18** 3249
[17] Hernandez W Y, Centeno M A, Romero-Sarria F and Odriozola J A 2009 *J. Phys. Chem.* C **113** 5629
[18] Kadowaki H, Saito N, Nishiyama H and Inoue Y 2007 *Chem. Lett.* **36** 440
[19] Andersson D A, Simak S I, Skorodumova N V, Abrikosov I A and Johansson B 2007 *Appl. Phys. Lett.* **90** 031909
[20] Yang Z, Luo G, Lu Z and Hermansson K 2007 *J. Chem. Phys.* **127** 074704
[21] Yang Z, Lu Z and Luo G 2007 *Phys. Rev.* B **76** 075421
[22] Shapovalov V and Metiu H 2007 *J. Catal.* **245** 205
[23] Wang X Q, Rodriguez J A, Hanson J C, Gamara D, Martinez-Arias A and Fernandez-Garcia M 2005 *J. Phys. Chem.* B **109** 19595
[24] Balducci G, Islam M S, Kaspar J, Fornasiero P and Graziani M 2000 *Chem. Mater.* **12** 677
[25] Wang H-F, Gong X-Q, Guo Y-L, Guo Y, Lu G Z and Hu P 2009 *J. Phys. Chem.* C **113** 10229
[26] Krishna K, Bueno-López A, Makkee M and Moulijn M A 2007 *Appl. Catal. B: Environ.* **75** 201

[27] Anisimov V I, Zaanen J and Andersen O K 1991 *Phys. Rev. B* **44** 943
[28] Dudarev S L, Botton G A, Savrasov S Y, Humphreys C J and Sutton A P 1998 *Phys. Rev. B* **57** 1505
[29] Castleton C W M, Kullgren J and Hermansson K 2007 *J. Chem. Phys.* **127** 244704
[30] Fabris S, Vicario G, Balducci G, de Gironcoli S and Baroni S 2005 *J. Phys. Chem. B* **109** 22860
[31] Henderson M A, Perkins C L, Engelhard M H, Thevuthasan S and Peden C H F 2003 *Surf. Sci.* **526** 1
[32] Kresse G and Hafner J 1994 *Phys. Rev. B* **49** 14251
Kresse G and Furthmüller J 1996 *Comput. Mater. Sci.* **6** 5
[33] Blöchl P E 1994 *Phys. Rev. B* **50** 17953
Joubert D and Kresse G 1999 *Phys. Rev. B* **59** 1758
[34] Perdew J P, Burke K and Ernzerhof M 1996 *Phys. Rev. Lett.* **77** 3865
[35] Tasker P W 1979 *J. Phys. C: Solid State Phys.* **12** 4977
[36] Schirmer O F 2006 *J. Phys.: Condens. Matter* **18** R667
[37] Stoneham A M, Gavartin J, Shluger A L, Kimmel A V, Munoz Ramo D, Ronnow H M, Aeppli G and Renner C 2007 *J. Phys.: Condens. Matter* **19** 255208
[38] Du M H and Zhang S B 2009 *Phys. Rev. B* **80** 115217
[39] Varnhorst T, Schirmer O F, Kroese H, Scharfschwerdt R and Kool Th W 1996 *Phys. Rev. B* **53** 116
[40] Cox R T 1971 *Solid State Commun.* **9** 1989
[41] Orera V M, Merino R I, Chen Y, Cases R and Alonso P J 1990 *Phys. Rev. B* **42** 9782
[42] Azzoni C B and Paleari A 1996 *Phys. Rev. B* **53** 5
[43] Stashans A and Bermeo S 2009 *Chem. Phys.* **363** 100

[44] Nolan M and Watson G W 2005 *Surf. Sci.* **586** 25
[45] Nolan M and Watson G W 2006 *J. Chem. Phys.* **125** 144701
[46] Laegsgaard J and Stokbro K 2002 *Phys. Rev. B* **65** 075208
[47] Pacchioni G, Frigoli F, Ricci D and Weil J A 2001 *Phys. Rev. B* **63** 054102
[48] Ghijsen J, Tjeng L H, van Elp J, Eskes H, Westerink J, Sawatzky G A and Czyzyk M T 1988 *Phys. Rev. B* **38** 11322
Elfimov I S, Yunoki S and Sawatzky G A 2002 *Phys. Rev. Lett.* **89** 216403
[49] Scanlon D O, Walsh A, Morgan B J, Nolan M, Fearon J and Watson G W 2007 *J. Phys. Chem. C* **111** 7971
[50] The binding energy of O_2 has been checked in a number of sources
Linde D R (ed) 1993 *CRC Handbook of Chemistry and Physics* (Boca Raton, FL: CRC Press)
West A R 1990 *Solid State Chemistry and its Applications* (New York: Wiley)
Douglas B E and McDaniel D H (ed) 1965 *Concepts and Models of Inorganic Chemistry* (New York: Wiley)
[51] Zinkevich M, Djurovic D and Aldinger F 2006 *Solid State Ion.* **177** 989
[52] Wu M C, Truong C M and Goodman D W 1992 *Phys. Rev. B* **46** 12688
[53] Ganduglia-Pirovano M V, Da Silva J L F and Sauer J 2009 *Phys. Rev. Lett.* **102** 026101
[54] Islam M M, Bredow T and Gerson A 2007 *Phys. Rev. B* **76** 045217
[55] Gesenhues U 2001 *J. Photochem. Photobiol.* A **139** 243